

UCSF

UC San Francisco Previously Published Works

Title

Gene Expression-based Molecular Scoring of Pancreas Transplant Rejection for a Quantitative Assessment of Rejection Severity and Resistance to Treatment

Permalink

<https://escholarship.org/uc/item/0np9p2zk>

Authors

Brown, Audrey E

Kelly, Yvonne M

Zarinsefat, Arya

et al.

Publication Date

2024-09-01

DOI

10.1016/j.ajt.2024.09.032

Peer reviewed













Contents lists available at ScienceDirect

American Journal of Transplantation

journal homepage: www.amjtransplant.org

Original Article

Gene expression–based molecular scoring of pancreas transplant rejection for a quantitative assessment of rejection severity and resistance to treatment

Audrey E. Brown^{1,†} , Yvonne M. Kelly^{1,2,†} , Arya Zarinsefat¹ ,
 Raphael P.H. Meier^{1,3} , Giulia Worner¹ , Mehdi Tavakol¹ , Minnie M. Sarwal¹ ,
 Zoltan G. Laszik¹ , Peter G. Stock^{1,*} , Tara K. Sigdel^{1,*} 

¹ Department of Surgery, University of California, San Francisco, California, USA² Department of Surgery, Columbia University, New York, New York, USA³ Department of Surgery, University of Maryland School of Medicine, Baltimore, Maryland, USA

ARTICLE INFO

Keywords:

pancreas transplant
 acute cellular rejection
 differential gene expression
 tissue Common Response
 Module score

ABSTRACT

Pancreas transplantation improves glycemic control and mortality in patients with diabetes but requires aggressive immunosuppression to control the alloimmune and autoimmune response. Recent developments in “omics” methods have provided gene transcript-based biomarkers for organ transplant rejection. The tissue Common Response Module (tCRM) score is developed to identify the severity of rejection in kidney, heart, liver, and lung transplants. Still, it has not yet been validated in pancreas transplants (PT). We evaluated the tCRM score’s relevance in PT and additional markers of acute cellular rejection (ACR) for PT. An analysis of 51 pancreas biopsies with ACR identified 37 genes and 56 genes significantly upregulated in the case of grade 3 and grade 2 ACR, respectively ($P < .05$). Significant differences were seen with higher grades of rejection among several transcripts. Of the 22 genes differentially expressed in grade 3 ACR, 18 were also differentially expressed in grade 2 ACR. The rejection signal was attributable to activated leukocytes’ infiltration. Significantly higher tCRM scores were found in grade 3 ACR ($P = .007$) and grade 2 ACR ($P = .004$), compared to normal samples. The tCRM score was able to distinguish treatment-resistant cases from those successfully treated for rejection.

Abbreviations: ACR, acute cellular rejection; AR, acute rejection; CRM, Common Response Module; DE, differential expression; FDR, false-discovery rate; FFPE, formalin-fixed paraffin-embedded; PA, pathway analysis; PT, pancreas transplant; PTA, pancreas transplant alone; QC, quality control; SPK, simultaneous pancreas and kidney; tCRM, tissue Common Response Module.

* Corresponding authors. 505 Parnassus Ave, M884A, 513 Parnassus Ave, HSE 520, San Francisco, CA, 94143, USA.

E-mail addresses: peter.stock@ucsf.edu (P.G. Stock), tara.sigdel@ucsf.edu (T.K. Sigdel).

† These authors contributed equally: Audrey E. Brown and Yvonne M. Kelly.

<https://doi.org/10.1016/j.ajt.2024.09.032>

Received 12 November 2023; Received in revised form 1 September 2024; Accepted 25 September 2024

1600-6135/© 2024 American Society of Transplantation & American Society of Transplant Surgeons. Published by Elsevier Inc. All rights are reserved, including those for text and data mining, AI training, and similar technologies.

1. Introduction

Since its inception, outcomes of pancreas transplantation continue to improve, often attributed to improved surgical technique, improved immunosuppression, and more standardized and rigorous selection of both donors and recipients.¹ Immunosuppression for pancreas transplants (PT) has evolved to more aggressive lymphodepleting induction regimens to control the alloimmune and autoimmune response. Despite these advances, acute rejection (AR) in the first year posttransplant continues to be a problem, with the most recent Organ Procurement Transplant Network and Scientific Registry of Transplant Recipients data showing rates of rejection in the first year of 12.5% for pancreas after kidney transplant, 21.8% for pancreas transplant alone (PTA), and 10.6% for the simultaneous pancreas and kidney (SPK) transplant.² Currently, the only method for assessing rejection is the image-guided biopsy of the allograft.^{3,4} A more quantitative assessment of the rejection episode could facilitate the decision of the aggressiveness of the treatment.

Recently, gene expression analysis-derived gene transcript panels have been explored as a tool to monitor molecular events related to graft injuries in solid organ transplantation.^{5,6} A few studies using targeted gene expression analysis on a limited set of gene transcripts were performed on peripheral blood^{7,8} and tissue.⁹ Several studies have used high-throughput transcriptome-level gene expression profiling to identify key immunologic and inflammatory markers in the blood and tissue of solid organ transplant recipients experiencing AR.¹⁰⁻¹⁴ These studies have been performed on solid organ transplants except PT. In one such study, gene expression analysis of public transcriptional data from kidney, heart, liver, and lung transplant recipients experiencing rejection was used to identify the tissue Common Response Module (tCRM) score based on 11 genes (*BASP1*, *ISG20*, *PSMB9*, *RUNX3*, *TAP1*, *NKG7*, *LCK*, *INPP5D*, *CXCL9*, *CD6*, and *CXCL10*; Khatri et al¹⁵). The tCRM score was shown to diagnose the severity of tissue rejection in all 4 graft types but has not yet been validated in PT.

This study aimed to evaluate the previously reported tCRM score^{15,16} in PT and identify any additional markers of PT-AR. Because both recurrent autoimmunity and alloimmunity contribute to the immune response following PT in people with type 1 diabetes, this study also aimed to unravel additional molecules associated with rejection in PT and the relevance of the tCRM score in predicting treatment response after PT rejection.

2. Materials and methods

2.1. Patient selection

This study was a retrospective, descriptive study approved by the institutional review board at the University of California, San Francisco (UCSF IRB approval number 19-28919). All available protocols and for-cause biopsies of PT at University of California, San Francisco from January 2006 to November 2018 were identified and used for this study. As a quality control (QC) measure, the formalin-fixed paraffin-embedded (FFPE) specimens were assessed for adequate RNA yield, with a total of 54 unique pancreas biopsies meeting the threshold. All the biopsies

were reclassified based on the most recent Banff classification schema.¹⁷ Three samples were excluded at the outset as they were each the only sample in their cohort—one with grade 4 acute cellular rejection (ACR), one with chronic rejection, and one with antibody-mediated rejection—bringing the final study total to 51 unique biopsies from 42 patients (Table 1). All 51 biopsies in the cluster were tested for C4d; all, except 2, were C4d negative. A single case in the “normal” group showed diffuse capillary endothelial C4d positivity and microvascular inflammation with donor-specific antibodies (DSA) positivity; this case has been excluded from the analysis. Clinical data collected included demographic data, operative data, details pertaining to episodes of rejection including the reason for biopsy and treatment administered, and dates of graft loss, and death (if applicable). Rejection that was resistant to treatment was defined as patients receiving 2 separate rounds of treatment less than 2 months apart. A detailed listing of biopsy scores and C4d data are presented in Supplementary Table 1.

2.2. Biopsy and management of rejection

For the vast majority of cases, biopsies were performed prior to treatment. However, due to timing and processing constraints, bolus steroids were initiated prior to a final biopsy result in a small number of patients. The standard protocol is to treat patients with mild ACR grade 1 with bolus steroids; however, thymoglobulin was also occasionally used as an initial treatment regimen when the treating physician felt the recipient was at a higher immunologic risk. The higher-risk patients included recipients with prior rejection or high baseline Panel-reactive antibodies (PRA). The initial treatments are included in Supplementary Table 1. Recurrent rejections were treated with thymoglobulin and/or Orthoclone (OKT3).

2.3. RNA isolation and gene expression

Total RNA was isolated using the Purelink FFPE RNA Isolation Kit (Invitrogen; Waltham, MA) from four 10 μm -thick FFPE sections for each sample. RNA yield (ng/ μL) and RNA purity (260/280 ratio) were measured using a Nanodrop 1000 Spectrophotometer (Thermo Fisher Scientific; Wilmington, DE). The median RNA yield per FFPE block was 31.01 ng/ μL (standard deviation [SD] = 23.82), with a median 260/280 value of 2.02 (SD = 0.22). Expression analysis of 760 immune response-related genes was performed on a NanoString nCounter Sprint Instrument (NanoString Technologies; Seattle, WA), based on the manufacturer's recommendations. Our gene panel (Supplementary Table 2) consisted of Nanostring's Cancer Immune v1.1 oligonucleotide set (n = 730), which includes 40 housekeeping genes, in addition to a custom panel of 30 probes and 40 housekeeping genes. Internal QC metrics of the platform were used with the default settings.¹⁸ As a QC metric, 2 duplicate samples were run in each category for grade 1 ACR, grade 2 ACR, and grade 3 ACR.

2.4. Gene expression analysis

Raw count data were imported into NanoString's nSolver software (v4.0) with the Advanced Analysis module, and R 3.3.2

Table 1
Patient information.

Case no.	Unique patient ID	Age at Txp (y)	Sex	Primary disease	Transplant type	Months post-Txp	Indication for biopsy	Pathology diagnosis
1	1	34	M	DM1	PAK	8	Cause, elevated glucose	No rejection
2	2	53	F	DM1	PTA	1	Cause, elevated glucose	ACR, grade 2
7	2	53	F	DM1	PTA	8	Cause, elevated amylase/lipase	ACR, grade 3
3	3	43	F	DM1	SPK	64	Cause, elevated amylase/lipase	ACR, grade 2
11	3	43	F	DM1	PTA ^a	1	Cause, elevated amylase/lipase	ACR, grade 2
22	3	43	F	DM1	PTA ^a	22	Cause, elevated amylase/lipase	ACR, grade 1
4	4	43	F	DM1	SPK	4	Cause, elevated amylase/lipase	ACR, grade 2
5	5	38	M	DM1	SPK	25	Cause, elevated amylase/lipase	ACR, grade 1
6	6	48	F	DM1	PTA	4	Protocol	ACR, grade 2
8	7	19	M	DM1	PTA	22	Cause, elevated amylase/lipase	ACR, grade 3
9	8	45	F	DM1	SPK	114	Cause, elevated amylase/lipase	ACR, grade 3
10	9	53	F	DM1	PTA	2	Protocol	ACR, grade 1
12	10	42	F	DM1	SPK	1	Cause, elevated amylase/lipase	ACR, grade 2
13	11	41	M	DM1	SPK	93	Cause, elevated amylase/lipase	ACR, grade 2
14	12	34	F	DM1/2	SPK	1	Cause, persistent fevers	ACR, grade 2
19	12	34	F	DM1/2	SPK	9	Cause, elevated amylase/lipase	No rejection
28	12	34	F	DM1/2	SPK	26	Cause, elevated amylase/lipase	No rejection
34	12	34	F	DM1/2	SPK	35	Cause, elevated amylase/lipase	No rejection (excluded from analysis)
15	13	38	M	DM1	SPK	4	Cause, elevated amylase/lipase	No rejection
16	14	41	F	DM1	PTA	28	Cause, elevated amylase/lipase	ACR, grade 3
25	14	41	F	DM1	PTA	45	Cause, elevated amylase/lipase	ACR, grade 1
17	15	38	M	DM1	SPK	133	Cause, elevated amylase/lipase	ACR, grade 3
18	16	29	F	DM1	PTA	12	Cause, elevated amylase/lipase	ACR, grade 2
20	17	49	F	DM1	SPK	1	Cause, elevated glucose	No rejection
21	18	32	M	DM1	SPK	10	Cause, elevated amylase/lipase	ACR, grade 2
23	19	49	F	DM1	SPK	12	Cause, elevated amylase/lipase	No rejection
24	20	48	M	DM1	PAK	2	Cause, elevated amylase/lipase	ACR, grade 2
26	21	49	F	DM1	SPK	11	Cause, elevated amylase/lipase	ACR, grade 1
27	21	49	F	DM1	SPK	12	Cause, elevated amylase/lipase	ACR, grade 1
30	21	49	F	DM1	SPK	13	Cause, elevated amylase/lipase	ACR, grade 3
29	22	43	M	DM1	SPK	63	Cause, elevated amylase/lipase	ACR, grade 3 (excluded from analysis)
31	23	40	M	DM1	PTA ^a	2	Protocol	No rejection
32	24	35	M	DM1	PAK	3	Protocol	No rejection
33	25	47	M		PTA	4	Cause, pain	ACR, grade 1

(continued on next page)

Table 1 (continued)

Case no.	Unique patient ID	Age at Txp (y)	Sex	Primary disease	Transplant type	Months post-Txp	Indication for biopsy	Pathology diagnosis
				Pancreatectomy after trauma				
35	26	40	M	DM1	SPK	1	Cause, persistent fevers	No rejection
36	27	36	M	DM1	SPK	1	Cause, persistent fevers	ACR, grade 1 (excluded from analysis)
37	28	51	F	DM1	PTA	9	Protocol	ACR, grade 1
38	29	41	F	DM1	PTA ^a	103	Cause, elevated glucose	ACR, grade 2
39	30	26	F	DM1	SPK	2	Cause, elevated amylase/lipase	No rejection
40	31	32	M	DM1	PAK	1	Cause, persistent fevers	ACR, grade 3
41	32	46	F	DM1	PTA	2	Protocol	ACR, grade 1
42	33	49	M	DM1	SPK	1	Cause, elevated amylase/lipase	No rejection
43	34	42	M	DM1	PAK	2	Cause, elevated glucose	ACR, grade 1
44	35	12	F	DM1	SPK	13	Cause, elevated amylase/lipase	No rejection
45	36	48	F	DM1	SPK	40	Cause, elevated amylase/lipase	ACR, grade 1
46	37	35	F	DM1	SPK	20	Cause, elevated amylase/lipase	ACR, grade 1
47	38	52	M	DM1	PTA ^a	2	Protocol	ACR, grade 3
48	39	36	F	DM1	SPK	13	Cause, elevated amylase/lipase	ACR, grade 2
49	40	38	M	DM1	SPK	40	Cause, elevated amylase/lipase	ACR, grade 1
50	41	53	M	DM1	SPK	11	Cause, elevated amylase/lipase	No rejection
51	42	40	M	DM1	SPK	49	Cause, elevated amylase/lipase	ACR, grade 2

ACR, acute cellular rejection; DM1, type 1 diabetes mellitus; DM1/2, mix of type 1 and type 2 diabetes mellitus; F, female; M, male; PAK, pancreas after kidney transplant; PTA, pancreas transplant alone; SPK, simultaneous pancreas and kidney; Txp, transplant.

^a Failed SPK s/p graft pancreatectomy.

(R Foundation for Statistical Computing; Vienna, Austria). The background noise threshold was determined to be 60 counts (calculated by taking the highest average count in the negative-control probe set, which was 30, and then doubling it, which resulted in 60). To ensure a strict cutoff for robust analysis and appropriate input data for differential expression (DE) analysis, any gene not expressed greater than the background noise threshold of 60 in at least 95% of the samples was excluded from downstream analysis. Gene counts were normalized based on a positive-control probe set (to adjust for technical variation) and the standard 40 housekeeping genes in the panel (to adjust for variation in RNA input). One sample from normal was excluded from the final analysis because of failing the criteria of being C4d and DSA positive. One sample from the grade 1 ACR cohort and one from the grade 3 ACR cohort were excluded from further analysis due to failure to detect a sufficient number of genes above the background. We performed DE analysis comparing normal pancreas to grade 1 ACR, normal vs grade 2 ACR, and normal vs grade 3 ACR.

For the analysis of the gene expression data set, DE analysis was performed in the Advanced Analysis module using a

negative binomial model. The Benjamini-Hochberg method was utilized to account for multiple comparison testing and calculate false-discovery rate (FDR) adjusted *P* values.¹⁹ We considered an adjusted *P* value < .05 to be statistically significant. The data were then exported to *R* for data visualization. The *pheatmap* package was utilized to perform unsupervised hierarchical clustering of all genes that had passed the raw count threshold cutoff.²⁰ Unsupervised clustering does not require any prior knowledge about the categories or labels of the data points such as gene transcripts or samples based on their expression patterns across the phenotypes, whereas supervised clustering was performed to visually display gene expression changes of select genes in known phenotypes. Z-scores were calculated for each normalized gene count for use in creating the heatmaps. The *ggplot2* package was used to create volcano plots in the standard fashion, plotting the log₂ fold changes against the -log₁₀ *P* values for each gene.²¹ All differentially expressed genes were plotted, with the 30 genes with the most significant adjusted *P* values labeled. The plots were colored based on whether each gene had an adjusted *P* value of less than or greater than .05.

2.4.1. Quantification of inflammation

To compare the amount of inflammation across biopsies and groups, we compared the expression level of protein tyrosine phosphatase, receptor type, C, also known as CD45, using the normalized gene counts. The gene counts in each group were compared using a Mann-Whitney test. We considered a P value $< .05$ to be statistically significant.

2.4.2. Comparison of tCRM gene expression

Using the log transformed gene counts for the 11 tCRM genes (*BASP1*, *ISG20*, *PSMB9*, *RUNX3*, *TAP1*, *NKG7*, *LCK*, *INPP5D*, *CXCL9*, *CD6*, and *CXCL1*), the tCRM score for each patient was calculated based on previously reported method¹⁵ and used to calculate the mean tCRM score for each pathologic group. The tCRM scores between groups were compared using a Mann-Whitney test. We considered a P value $< .05$ to be statistically significant.

2.4.3. Correlation between tCRM score and amylase values

A Pearson correlation was performed to assess the significance between the tCRM scores and time-matching amylase values. Survival analyses were performed using the Kaplan-Meier method and log-rank test.

2.4.4. ROC analysis to compare performance of tCRM score, lipase, and amylase values

A receiver operating characteristic (ROC) analysis was performed to compare the utility of tCRM scores to lipase and amylase values.

2.4.5. Pathway analysis

Genes from DE analysis, as described above, were then filtered for all genes with adjusted P values $< .05$ and \log_2 fold

changes greater than 0.5 to 1.0. These genes were then input to the packages *clusterProfiler* and *ReactomePA* to perform Reactome pathway analysis (PA).^{22,23} The results of the PA were then visualized as bar plots, and ordered by the adjusted P values that were calculated for each individual pathway in the PA.

A summary of the study design is presented in Figure 1.

3. Results

3.1. Patient demographics

A total of 51 unique patient biopsies from 42 patients were included in our initial data set with the following histopathologic diagnoses: 14 normal biopsies, 14 grade 1 ACR, 14 grade 2 ACR, and 9 grade 3 ACR (Table 1). Of the 42 unique patients, 21 were men (50%). Age at the time of transplant ranged from 12 to 53 years, with the average age being 40.5 years. Time from transplant to biopsy ranged from 1 to 133 months with the average time being 22 months. One patient had a total pancreatectomy after trauma. Twenty-five patients (59.5%) underwent SPK transplant, 5 (11.9%) underwent pancreas after kidney transplant, and 12 (28.5%) underwent PTA. Of those who underwent PTA, 3 of the 12 had a prior SPK transplant with subsequent pancreatectomy due to graft failure. The indications for biopsies were: (1) elevated amylase and/or lipase, 25 patients (59.5%); (2) standard protocol biopsy, 7 patients (16.7%); (3) elevated glucose, 5 patients (11.9%); (4) persistent fever, 4 patients (9.5%); and (5) graft pain, 1 patient (2.4%).

3.2. Transcriptional differences with increasing grades of rejection

A total of 188 genes out of 760 genes included in the nCounter platform (Supplementary Table 2) met the raw count cutoff

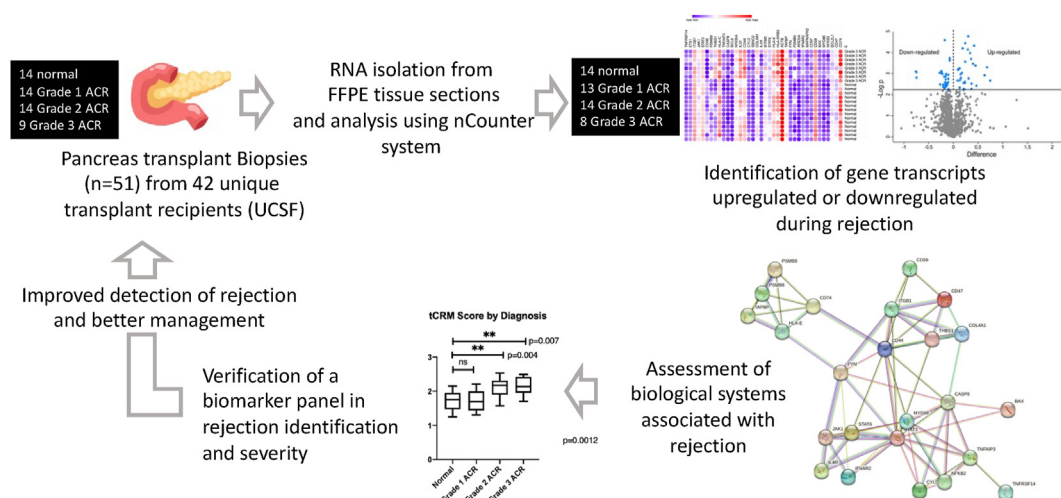


Figure 1. Study schematic. Pancreas transplant biopsies ($n = 51$) preserved as formalin-fixed paraffin-embedded (FFPE) blocks were assessed for gene expression changes for different grades of biopsy-proven rejection at the time of rejection by comparing it with gene expression in normal nonrejecting controls. We identified several genes associated with rejection and impacted biological processes due to the rejection. We also tested the utility of a previously published set of 11 gene transcripts known as Common Response Module genes and performed an analysis of correlating Common Response Module scores with the severity of rejection. ACR, acute cellular rejection; tCRM, tissue Common Response Module; UCSF, University of California, San Francisco.

thresholds described above and were included in our analysis. We ran individual comparisons of normal biopsies ($n = 13$) against biopsies with grade 1 ACR ($n = 13$), grade 2 ACR ($n = 14$), and grade 3 ACR ($n = 8$). No significant differences in gene expression were seen when comparing grade 1 ACR to normal samples. To understand and capture subtle differences in grade 1 ACR compared to normal, we used a simple unpaired t-test P value $< .1$ as a cutoff threshold. This approach resulted in SMAD3, HMGB1, MAP2K1, RORA, ITCH, LTBR, NFKB2, CD44, FOS, IGF2R being significant. These genes are enriched in biological processes such as regulation of tolerance induction (FDR < 0.022) and myeloid dendritic cell activation FDR (< 0.027).

Unsupervised hierarchical clustering of all 188 genes revealed ACR-specific clustering by phenotype for the normal vs grade 2 ACR as 8 out of 14 ACR grade 2 samples were clustered together (Fig. 2A) and normal vs grade 3 ACR as 6 out of 8 ACR grade 3 samples were clustered together (Fig. 2B) but not for normal vs grade 1 ACR (not shown). The clustering demonstrated a potential sampling bias in the tissue used for gene expression assay and histologic grading. To better display the spread of the most significantly upregulated genes, we used volcano plots for normal vs grade 3 ACR (Fig. 2C) and normal vs grade 2 ACR (Fig. 2D). Significant differences in gene expression were found when comparing grade 2 and grade 3 ACR to normal samples using DE analysis. Fifty-six genes were differentially expressed in grade 2 ACR (Table 2) and 37 genes were differentially expressed in grade 3 ACR (Table 3), compared with normal samples.

Among these genes with significantly higher expression, 15 in the grade 3 ACR group and 24 in the grade 2 ACR group had a

\log_2 fold-change > 1.0 in gene expression. The top 10 genes increased in grade 2 ACR group in terms of their fold increase included APOE, FN1, AMBP, HLA-DRB3, MX1, THBS1, CD74, PSMB9, C3, and STAT1. The top 10 genes in grade 3 ACR group in terms of their fold increase were THBS1, CD44, HLA-DRB3, IL32, PSMB9, CD74, COL4A1, TNFAIP3, TAPBP, and NFKB2. Among the top transcripts by fold-change, 8 genes were found to be highly expressed in both the grade 3 and grade 2 ACR groups compared to normal: ARID5A, CD44, CD74, COL4A1, HLA-DRB3, NFKB2, PSMB9, TAPBP, and THBS1.

A heatmap with supervised clustering shows the similarity and differences in gene expression values between grade 2 ACR vs normal (Fig. 3A) and grade 3 ACR vs normal (Fig. 3B). Among the upregulated genes in both grade 2 ACR and grade 3 ACR, 28 genes were upregulated in both grades of ACR (Fig. 3C). A PA of these genes demonstrated significant enrichment of a number of biological processes. The top 2 processes were the immune system process (FDR $1.47E-16$) and response to cytokine (FDR $4.67E-16$) (Fig. 3D).

A PA was performed on the genes that were significantly differentially expressed with adjusted P value $< .05$ and demonstrated a \log_2 fold-change > 1.0 in gene expression (Fig. 4A). This showed that genes enriched in the ACR groups tended to be part of inflammatory pathways such as interferon signaling, antigen processing and presentation, and phagocytosis. In a separate analysis, we analyzed 69 gene transcripts that increased in grade 2 ACR alone, grade 3 ACR alone, or both. The top 3 enriched molecular networks were responses to cytokines, immune system processes, and the immune system (Fig. 4B).

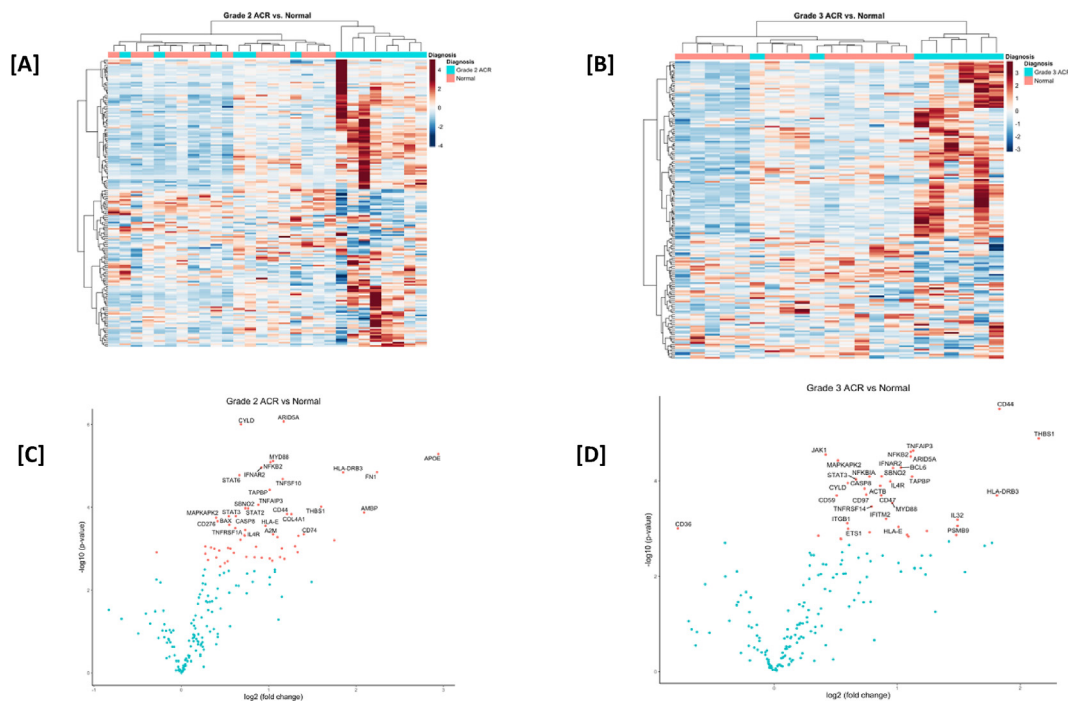


Figure 2. Gene expression analysis of pancreas transplants identifies genes associated with ACR 2 and ACR3 rejection grades. Unsupervised hierarchical clustering of all 188 genes comparing grade 2 acute cellular rejection (ACR) and normal biopsies (A) and comparing grade 3 ACR and normal biopsies (B). Differential expression analysis plotted as volcano plots comparing grade 2 acute cellular rejection (ACR) and normal biopsies (C) and comparing grade 3 ACR and normal biopsies (D).

Table 2

Significantly increased gene transcripts in acute cellular rejection grade 2.

Gene ID	Gene name	Log ₂ fold-change	Adjusted P value ^a
APOE	Apolipoprotein E (APOE)	2.94	.002
FN1	Fibronectin 1 (FN1)	2.24	.002
AMBP	Alpha-1-microglobulin/bikunin precursor (AMBP)	2.09	.009
HLA-DRB3	Major histocompatibility complex, class II, DR beta 3	1.85	.002
MX1	MX dynamin like GTPase 1 (MX1)	1.75	.020
THBS1	Thrombospondin 1 (THBS1)	1.6	.008
CD74	CD74 molecule (CD74)	1.4	.017
PSMB9	Proteasome 20S subunit beta 9 (PSMB9)	1.34	.017
C3	Complement C3 (C3)	1.33	.029
STAT1	Signal transducer and activator of transcription 1 (STAT1)	1.3	.026
COL4A1	Collagen type IV alpha 1 chain (COL4A1)	1.26	.009
CD44	CD44 molecule (Indian blood group) (CD44)	1.21	.009
HLA-DRA	Major histocompatibility complex, class II, DR alpha (HLA-DRA)	1.18	.036
ARID5A	AT-rich interaction domain 5A (ARID5A)	1.17	.001
TNFSF10	TNF superfamily member 10 (TNFSF10)	1.16	.002
C1S	Complement C1s (C1S)	1.15	.026
HLA-DMA	Major histocompatibility complex, class II, DM alpha	1.13	.034
HLA-A	Major histocompatibility complex, class I, A (HLA-A)	1.1	.018
MYD88	MYD88 innate immune signal transduction adaptor	1.05	.002
A2M	Alpha-2-macroglobulin (A2M)	1.05	.017
HLA-B	Major histocompatibility complex, class I, B	1.04	.038
NFKB2	Nuclear factor kappa B subunit 2 (NFKB2)	1.02	.002
TAPBP	TAP binding protein (TAPBP)	1.01	.004
C1R	Complement C1r (C1R)	1.01	.036
HLA-E	Major histocompatibility complex, class I, E(HLA-E)	0.962	.013
PSMB8	Proteasome 20S subunit beta 8 (PSMB8)	0.92	.034
IFNAR2	Interferon alpha and beta receptor subunit 2 (IFNAR2)	0.916	.002
TNFAIP3	TNF alpha induced protein 3 (TNFAIP3)	0.88	.008
IFIH1	Interferon induced with helicase C domain 1 (IFIH1)	0.854	.026
SERPING1	Serpin family G member 1 (SERPING1)	0.838	.034
STAT2	Signal transducer and activator of transcription 2 (STAT2)	0.765	.008
ITGA1	Integrin subunit alpha 1 (ITGA1)	0.743	.034
SBNO2	Strawberry notch homolog 2 (SBNO2)	0.733	.008
IL4R	Interleukin 4 receptor (IL4R)	0.731	.015
JAK2	Janus kinase 2 (JAK2)	0.726	.017
FYN	FYN proto-oncogene, Src family tyrosine kinase (FYN)	0.721	.017
CYLD	CYLD lysine 63 deubiquitinase (CYLD)	0.683	.001
CD47	CD47 molecule (CD47)	0.677	.020

(continued on next page)

Table 2 (continued)

Gene ID	Gene name	Log ₂ fold-change	Adjusted P value ^a
STAT6	Signal transducer and activator of transcription 6 (STAT6)	0.663	.002
CASP8	Caspase 8 (CASP8)	0.623	.009
TNFRSF1A	TNF receptor superfamily member 1A (TNFRSF1A)	0.616	.014
TNFRSF14	TNF receptor superfamily member 14 (TNFRSF14)	0.601	.030
IL13RA1	Interleukin 13 receptor subunit alpha 1 (IL13RA1)	0.56	.026
BAX	BCL2 associated X, apoptosis regulator (BAX)	0.549	.013
STAT3	Signal transducer and activator of transcription 3 (STAT3)	0.543	.009
GAPDH	Glyceraldehyde-3-phosphate dehydrogenase (GAPDH)	0.534	.026
ENG	Endoglin (ENG)	0.53	.038
ICAM3	Intercellular adhesion molecule 3 (ICAM3)	0.498	.042
ITGB1	Integrin subunit beta 1 (ITGB1)	0.446	.050
IKBKB	Inhibitor of nuclear factor kappa B kinase subunit beta (IKBKB)	0.433	.028
CD276	CD276 molecule (CD276)	0.415	.011
NFATC2	Nuclear factor of activated T cells 2 (NFATC2)	0.399	.034
MAPKAPK2	MAPK activated protein kinase 2 (MAPKAPK2)	0.397	.009
CD59	CD59 molecule (CD59 blood group) (CD59)	0.377	.026
SMAD3	SMAD family member 3 (SMAD3)	0.339	.026
ATG7	Autophagy related 7 (ATG7)	0.305	.037
JAK1	Janus kinase 1 (JAK1)	0.274	.026
CHUK	Component of inhibitor of nuclear factor kappa B kinase complex (CHUK)	0.274	.031

^a P values adjusted using the Benjamini-Hochberg correction.

3.3. Increased inflammation with increasing grades of rejection

Mean raw counts of protein tyrosine phosphatase, receptor type, C, also known as CD45, were compared across groups. The mean and SD of raw counts were as follows: grade 3 ACR 266 ± 146, grade 2 ACR 246 ± 164, grade 1 ACR 81 ± 82, and normal 78 ± 37. Overall analysis of variance (ANOVA) found a statistical difference between groups with $P = .0001$. A pairwise comparison was performed with statistically significant differences in CD45 expression between grade 3 ACR and normal ($P = .002$), grade 2 ACR and normal ($P = .003$), grade 3 ACR and grade 1 ACR ($P = .001$), and grade 2 ACR and grade 1 ACR ($P = .001$) (Fig. 5A).

3.4. tCRM score correlated with rejection grades and amylase levels, and ROC analysis demonstrated that the tCRM score performs better than the conventional markers (lipase and amylase) in distinguishing ACR from normal tissue

The tCRM score for each patient was calculated using transcript counts for the 11 Common Response Module (CRM) genes. The tCRM score between grade 3 ACR vs normal ($P = .0034$) and grade 2 ACR vs normal was statistically significant (P

$= .0023$) (Fig. 5B). tCRM scores of grade 2 ACR and grade 3 ACR were significantly higher compared to the tCRM score of grade 1 ACR with P values of .004 and .01, respectively. There was a significant correlation between the tCRM scores and captured amylase data at the time of biopsy ($P = .024$, $r = 0.33$).

Using tCRM scores the area under the curve (AUC) was 0.71 ($P = .02$) to differentiate AR from normal tissue. With a tCRM score cutoff of 1.83, the sensitivity and specificity to detect AR were 71% and 57%, respectively. When the same approach was tested with lipase, the AUC was 0.52 ($P = .89$) to differentiate from normal tissue. With a lipase (log base 2) cutoff of 6.9, the sensitivity and specificity to detect AR were 54% and 43%, respectively. With amylase, the AUC was 0.52 ($P = .86$) to identify ACR grade 2 and 3 from normal tissues. With an amylase (log base 2) cutoff of 7.6, the sensitivity and specificity to detect ACR grade 2 and 3 were 50% and 33%, respectively (Supplementary Fig. S1).

3.5. tCRM score correlates with rejection that is resistant to treatment

Of the 49 samples included in the analysis, 35 were collected at the time of the ACR event. Treatments administered for each included episode of rejection were pulse-dose methylprednisolone in 14 patients, thymoglobulin in 17 patients, OKT3

Table 3

Significantly increased gene transcripts in acute cellular rejection grade 3.

Gene symbol	Gene name	Log ₂ fold-change	Adjusted P value ^a
THBS1	Thrombospondin 1 (THBS1)	2.15	.006
CD44	CD44 molecule (Indian blood group) (CD44)	1.83	.003
HLA-DRB3	Major histocompatibility complex, class II, DR beta 3 (HLA-DRB3)	1.81	.011
IL32	Interleukin 32 (IL32)	1.49	.029
PSMB9	Proteasome 20S subunit beta 9 (PSMB9)	1.49	.036
CD74	CD74 molecule (CD74)	1.48	.044
COL4A1	Collagen type IV alpha 1 chain (COL4A1)	1.24	.040
TNFAIP3	TNF alpha induced protein 3 (TNFAIP3)	1.13	.006
TAPBP	TAP binding protein (TAPBP)	1.12	.007
NFKB2	Nuclear factor kappa B subunit 2 (NFKB2)	1.11	.006
ARID5A	AT-rich interaction domain 5A (ARID5A)	1.11	.006
PSMB8	Proteasome 20S subunit beta 8 (PSMB8)	1.09	.045
HLA-C	Major histocompatibility complex, class I, C (HLA-C)	1.08	.044
BCL6	BCL6 transcription repressor (BCL6)	1.03	.007
HLA-E	Major histocompatibility complex, class I, E (HLA-E)	1.01	.036
IFNAR2	Interferon alpha and beta receptor subunit 2 (IFNAR2)	0.97	.007
MYD88	MYD88 innate immune signal transduction adaptor (MYD88)	0.96	.015
IL4R	Interleukin 4 receptor (IL4R)	0.94	.008
IFITM2	Interferon induced transmembrane protein 2 (IFITM2)	0.91	.029
SBNO2	Strawberry notch homolog 2 (SBNO2)	0.87	.007
CD47	CD47 molecule (CD47)	0.87	.011
ACTB	Actin beta (ACTB)	0.86	.009
TNFRSF14	TNF receptor superfamily member 14 (TNFRSF14)	0.79	.016
FYN	FYN proto-oncogene, Src family tyrosine kinase (FYN)	0.78	.041
NFKBIA	NFKB inhibitor alpha (NFKBIA)	0.77	.007
CD97	Leukocyte antigen CD97 (CD97)	0.75	.011
CASP8	Caspase 8 (CASP8)	0.73	.009
STAT3	Signal transducer and activator of transcription 3 (STAT3)	0.66	.008
ETS1	ETS proto-oncogene 1, transcription factor (ETS1)	0.60	.037
CYLD	CYLD lysine 63 deubiquitinase (CYLD)	0.60	.008
ITGB1	Integrin subunit beta 1 (ITGB1)	0.59	.032
BAX	BCL2 associated X, apoptosis regulator (BAX)	0.54	.048
STAT6	Signal transducer and activator of transcription 6 (STAT6)	0.54	.048
MAPKAPK2	MAPK activated protein kinase 2 (MAPKAPK2)	0.52	.006
CD59	CD59 molecule (CD59 blood group) (CD59)	0.51	.011
JAK1	Janus kinase 1 (JAK1)	0.42	.006
BCL2L1	BCL2 like 1 (BCL2L1)	0.36	.044

^a P values adjusted using the Benjamini-Hochberg correction.

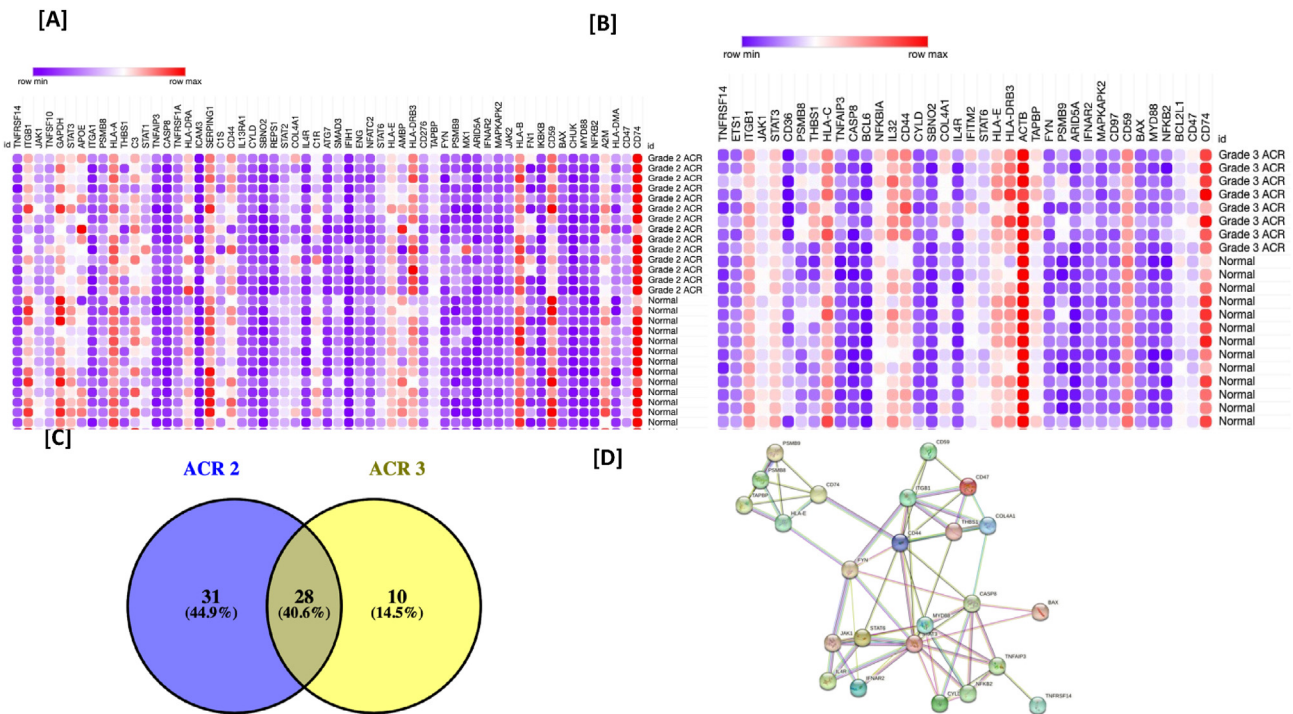


Figure 3. Common and unique gene transcripts specific to rejection severity and biological processes involved with rejection. A supervised clustering lists 58 and 37 genes significantly changed in ACR2 (A) and ACR3 (B), 28 genes overlapped as shown in Venn diagram (C). The common genes significantly changed in acute cellular rejection (ACR) grades 2 and 3 were enriched in biological processes such as the immune system process (false-discovery rate, 1.47E-16) and response to cytokine (false-discovery rate, 4.67E-16) (D).

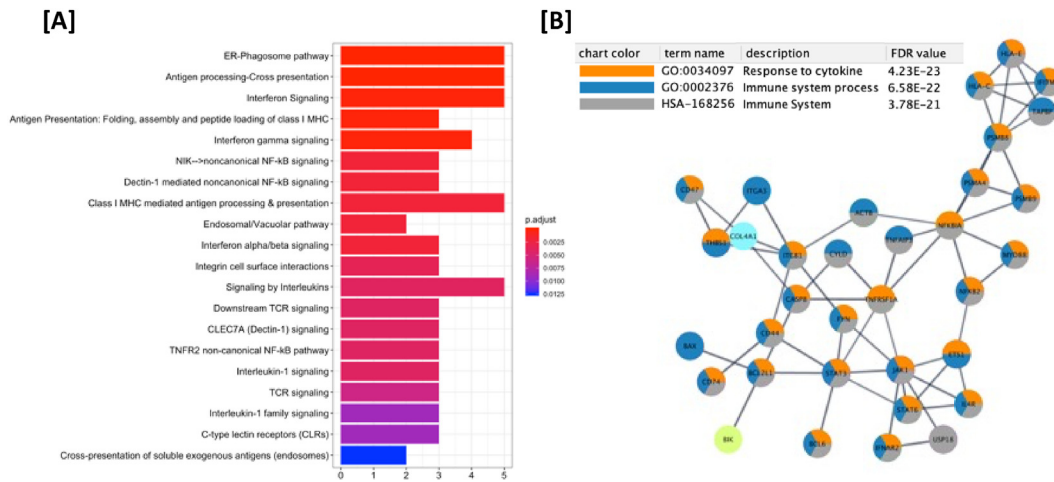


Figure 4. Pathway analysis enriched biological processes. Pathway analysis was performed on the genes that were significantly differentially expressed and demonstrated a log₂ fold-change > 1.0 comparing grade 3 acute cellular rejection (ACR) and normal biopsies (Fig. 3A) and comparing grade 2 ACR and normal biopsies. ER-phagosome pathway, antigen processing-cross presentation, and interferon signaling were among the top processes enriched (A). In a separate analysis, we analyzed 69 gene transcripts that increased in grade 2 ACR and grade 3 ACR. A molecular network with enrichment of processes such as response to cytokine, immune system process, and immune system are the top 3 processes enriched (B). FDR, false-discovery rate.

monoclonal antilymphocyte antibody in 2 patients, and escalation of immunotherapy in 2 patients. Patients with rejection who were resistant to treatment (defined as the receipt of second-line treatment within 2 months of initial diagnosis) had significantly higher tCRM scores than those who were successfully treated with first-line therapy (Fig. 6A). When stratified by pathologic grade, a statistically significant difference in tCRM scores

persisted in patients with grade 1 ACR but was not seen in those with grade 2 or grade 3 ACR (Fig. 6B). Of the patients who were resistant to treatment, 3 initially received thymoglobulin followed by OKT3, 2 initially received OKT3 followed by a second round of OKT3, and 1 initially received pulse-dose methylprednisolone followed by pancreatotomy. The Kaplan-Meier analysis survival rate at 7 years posttransplant revealed favorable graft survival

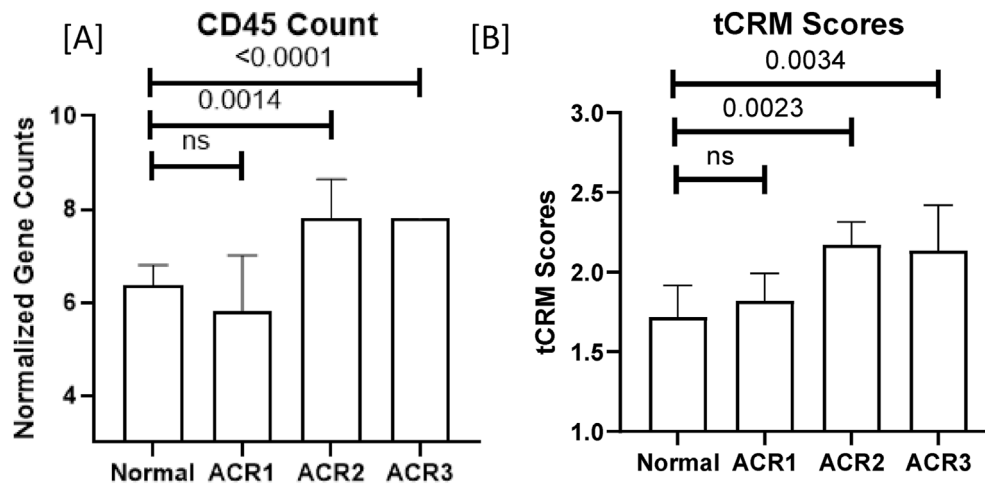


Figure 5. Quantification of inflammation by CD45 expression and the tissue Common Response Module (tCRM) score. A pairwise comparison was performed with statistically significant differences in CD45 expression between grade 3 acute cellular rejection (ACR) and normal ($P < .0001$), grade 2 ACR and normal ($P = .0014$), (A). The tCRM score identifies grade 3 ACR vs normal ($P = .0034$) and grade 2 ACR vs normal ($P = .0023$) (B).

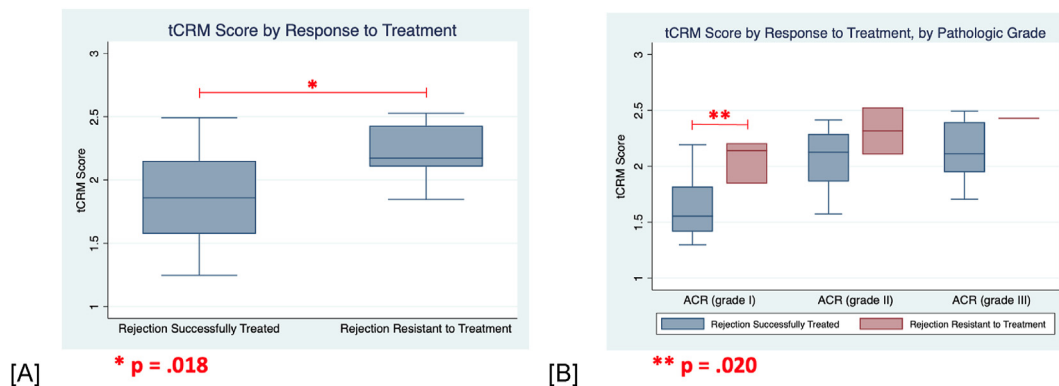


Figure 6. The tissue Common Response Module (tCRM) score by the response to treatment for acute cellular rejection (ACR) rejection. A pairwise comparison was performed with statistically significant differences in tCRM scores for patients with successfully treated rejection compared with those with rejection resistant to treatment ($P = .018$) (A). When stratified by pathologic grade, a significant difference in tCRM scores was seen in grade 1 ACR ($P = .02$), but not within grade 2 or grade 3 ACR (B).

outcomes with grafts with tCRM score < 2.1 in our cohort (Supplementary Fig. S2). The difference in survival rates between pancreas grafts with low vs high tCRM scores highlights the importance of tCRM assessment.

4. Discussion

Pancreas transplantation outcomes have steadily improved over the past 40 years. However, acute pancreas allograft rejection continues to pose a clinical challenge and is the primary cause of death-censored pancreas allograft loss after 3 months posttransplant.¹ In this first-of-its-kind study in pancreas transplantation, we report significantly different gene expression patterns and associated biological pathways in pancreas biopsies of patients with grade 2 and grade 3 ACR compared with normal samples. By taking a more focused approach with a clinically translatable gene panel, we analyzed tCRM gene transcripts. We found that the tCRM score correlates with the Banff histologic grading criteria and may identify patients at risk for treatment-resistant rejection. CRM gene set was identified using

a meta-analysis approach on publicly available high-throughput gene expression data.¹⁵ The tCRM score (CRM score for tissues) has been demonstrated as a robust biomarker for transplant rejection in multiple organs that include kidney tissue^{11,13,16,24} of kidney transplant recipients, urine of kidney transplant recipients,²⁵ lung transbronchial brushings, broncho-alveolar lavage, and lung explant.¹² The 11 CRM genes have been reported to be expressed in B cells,²⁶ NK cells^{27,28} and T cells.²⁹

Diagnosis and treatment of acute pancreas allograft rejection continue to be a challenge. Pancreas allograft rejection is typically asymptomatic, which means laboratory markers like serum amylase, lipase, and glucose are critical to the early identification of possible rejection. The same laboratory abnormalities can be seen in a number of other pathologies, however, including large vessel thrombosis, recurrence of autoimmune disease, islet cell drug toxicity, and chronic rejection or graft sclerosis. This makes tissue biopsy necessary for diagnosis,³⁰ with most centers using the Banff histologic grading criteria which were initially published in 2008 and continue to be widely used.³¹

Despite consensus on histologic grading criteria, there continues to be debate on treatment paradigms for patients with acute allograft rejection. As with rejection following any solid organ transplant, adequate treatment of the rejection episode must be balanced with an increased risk of infection from increased immunosuppression. A recently published single center report demonstrated that 83% of patients with grade 1 ACR will be adequately treated with pulse-dose steroids, whereas those with grade 2 and grade 3 ACR experienced better graft survival when treated with thymoglobulin.³² Of the 17% of patients with grade 1 ACR who were resistant to treatment with steroids, more than half ultimately required thymoglobulin to treat their rejection. Our findings suggest that the tCRM score may be able to identify patients, particularly those with grade 1 ACR, who have more aggressive rejection than would be diagnosed based on histologic findings alone, and thus warrant more aggressive initial treatment regimens.

Limitations of this study include a relatively small sample size and the inclusion of samples from a single center. Given the paucity of data focused on pancreas-specific allograft rejection, significant center-to-center variation exists with regard to allograft monitoring and rejection treatment protocols. Similarly, the samples included in this study were collected between 2006 and 2018, and even within our center, multiple changes have been made to the management of our immunosuppression, biopsy protocols, and treatment regimens during this time period. The use of FFPE in assessing transcriptome poses some issues with fragmented RNA, which might have contributed to damping down the signal reflected in no significant difference between ACR grade 1 vs no rejection. Antibody-mediated rejection has been increasingly recognized in pancreas allografts but was excluded from this analysis due to an insufficient number of samples. Lastly, we were not able to perform independent validation of the study results except for validation of the tCRM gene score, which validates the assay and the strategy overall.

In summary, increased access to gene expression data in blood^{7,8,33} and biopsy⁷ from PT recipients, including the data presented in this report, provides a much-needed means of AR detection and management by consolidating conventional diagnostic methods and subclassifying PT recipients based on resistance to rejection therapy. This study profiled rejection-specific gene transcripts in pancreas transplantation and that tCRM score, significant in transplant rejection in other solid organ transplants^{11-13,16,24,25} was also highly informative for diagnosing and quantifying AR injury in PT. Longitudinally assessing tCRM scores would provide clinically relevant signals about long-term outcomes and graft failure.

Acknowledgments

The authors acknowledge significant support from Dr Milan Bimali, PhD, from the Department of Biostatistics, University of Arkansas for Medical Sciences, during revision.

Funding

This work was supported in part by the NIH: 5 T32 AI 125222 (A.E.B., Y.M.K., and A.Z.) and by a Jon Fryer Resident Scientist

Scholarship from the American Society of Transplant Surgeons (A.E.B. and Y.M.K.).

Declaration of competing interest

The authors of this manuscript have no conflicts of interest to disclose as described by the American Journal of Transplantation.



Data availability

The data that support the findings of this study are available on request from the corresponding author. The data are not publicly available due to privacy or ethical restrictions.

Appendix A. Supplementary data

Supplementary data to this article can be found online at <https://doi.org/10.1016/j.ajt.2024.09.032>.

ORCID

Audrey E. Brown  <https://orcid.org/0000-0002-6898-2114>
 Yvonne M. Kelly  <https://orcid.org/0000-0002-1494-0429>
 Arya Zarinsefat  <https://orcid.org/0000-0001-8933-934X>
 Raphael P.H. Meier  <https://orcid.org/0000-0001-9050-0436>
 Giulia Worner  <https://orcid.org/0009-0008-9932-1061>
 Mehdi Tavakol  <https://orcid.org/0000-0002-2870-2544>
 Minnie M. Sarwal  <https://orcid.org/0000-0003-1212-3959>
 Zoltan G. Laszik  <https://orcid.org/0000-0003-0511-8764>
 Peter G. Stock  <https://orcid.org/0000-0002-5806-0167>
 Tara K. Sigdel  <https://orcid.org/0000-0001-8448-0328>

References

- Parajuli S, Djamali A, Mandelbrot D, et al. The presence of donor-specific antibodies around the time of pancreas graft biopsy with rejection is associated with an increased risk of graft failure. *Transplantation*. 2022; 106(6):e289–e296. <https://doi.org/10.1097/TP.0000000000004133>.
- Kandaswamy R, Stock PG, Miller J, et al. OPTN/SRTR 2020 annual data report: pancreas. *Am J Transplant*. 2022;22(suppl 2):137–203. <https://doi.org/10.1111/ajt.16979>.
- Lee BC, McGahan JP, Perez RV, Boone JM. The role of percutaneous biopsy in detection of pancreatic transplant rejection. *Clin Transplant*. 2000;14(5):493–498. <https://doi.org/10.1034/j.1399-0012.2000.140508.x>.
- Klassen DK, Weir MR, Cangro CB, Bartlett ST, Papadimitriou JC, Drachenberg CB. Pancreas allograft biopsy: safety of percutaneous biopsy—results of a large experience. *Transplantation*. 2002;73(4): 553–555. <https://doi.org/10.1097/00007890-200202270-00011>.
- Sarwal MM, Sigdel TK, Salomon DR. Functional proteogenomics—embracing complexity. *Semin Immunol*. 2011;23(4): 235–251. <https://doi.org/10.1016/j.smim.2011.08.002>.
- Bestard O, Cruzado JM, la Franquesa M, Grinyó JM. Biomarkers in renal transplantation. *Curr Opin Organ Transplant*. 2010;15(4):467–473. <https://doi.org/10.1097/MOT.0b013e32833b9ccb>.
- Cashion A, Sabek O, Driscoll C, Gaber L, Kotb M, Gaber O. Correlation of genetic markers of rejection with biopsy findings following human pancreas transplant. *Clin Transplant*. 2006;20(1):106–112. <https://doi.org/10.1111/j.1399-0012.2005.00450.x>.
- Cashion AK, Sabek OM, Driscoll CJ, Gaber LW, Gaber AO. Serial peripheral blood cytotoxic lymphocyte gene expression measurements for prediction of pancreas transplant rejection. *Transplant Proc*. 2006; 38(10):3676–3677. <https://doi.org/10.1016/j.transproceed.2006.10.113>.

9. Luan FL, Trillsch F, Henger A, et al. A pilot study of gene expression-based categorization of pancreas transplant biopsies. *Transplantation*. 2009;87(2):222–226. <https://doi.org/10.1097/TP.0b013e31818c88fbf>.
10. Nasr M, Sigdel T, Sarwal M. Advances in diagnostics for transplant rejection. *Expert Rev Mol Diagn*. 2016;16(10):1121–1132. <https://doi.org/10.1080/14737159.2016.1239530>.
11. Sigdel TK, Nguyen M, Dobi D, et al. Targeted transcriptional profiling of kidney transplant biopsies. *Kidney Int Rep*. 2018;3(3):722–731. <https://doi.org/10.1016/j.ekir.2018.01.014>.
12. Sacreas A, Yang JYC, Vanaudenaerde BM, et al. The common rejection module in chronic rejection post lung transplantation. *PLoS One*. 2018; 13(10):e0205107. <https://doi.org/10.1371/journal.pone.0205107>.
13. Zarinsfat A, Guerra JMA, Sigdel T, et al. Use of the tissue common rejection module score in kidney transplant as an objective measure of allograft inflammation. *Front Immunol*. 2020;11:614343. <https://doi.org/10.3389/fimmu.2020.614343>.
14. Vitalone MJ, Sigdel TK, Salomonis N, Sarwal RD, Hsieh SC, Sarwal MM. Transcriptional perturbations in graft rejection. *Transplantation*. 2015;99(9):1882–1893. <https://doi.org/10.1097/TP.0000000000000809>.
15. Khatri P, Roedder S, Kimura N, et al. A common rejection module (CRM) for acute rejection across multiple organs identifies novel therapeutics for organ transplantation. *J Exp Med*. 2013;210(11): 2205–2221. <https://doi.org/10.1084/jem.20122709>.
16. Sigdel TK, Bestard O, Tran TQ, et al. A computational gene expression score for predicting immune injury in renal allografts. *PLoS One*. 2015; 10(9):e0138133. <https://doi.org/10.1371/journal.pone.0138133>.
17. Drachenberg CB, Buettner-Herold M, Aguiar PV, et al. Banff 2022 pancreas transplantation multidisciplinary report: refinement of guidelines for T cell-mediated rejection, antibody-mediated rejection and islet pathology. Assessment of duodenal cuff biopsies and noninvasive diagnostic methods. *Am J Transplant*. 2024;24(3):362–379. <https://doi.org/10.1016/j.ajt.2023.10.011>.
18. Adam B, Afzali B, Dominy KM, et al. Multiplexed color-coded probe-based gene expression assessment for clinical molecular diagnostics in formalin-fixed paraffin-embedded human renal allograft tissue. *Clin Transplant*. 2016;30(3):295–305. <https://doi.org/10.1111/ctr.12689>.
19. Benjamini Y, Yekutieli D. The control of the false discovery rate in multiple testing under dependency. *Ann Statist*. 2001;29(4):1165–1188. <https://doi.org/10.1214/aos/1013699998>.
20. Kolde R. pheatmap: Pretty Heatmaps. <https://cran.r-project.org/web/packages/pheatmap/pheatmap.pdf>; 2019. Accessed November 5, 2022.
21. Wickham H. *ggplot2: Elegant Graphics for Data Analysis*. Springer; 2016.
22. Yu G, Wang LG, Han Y, He QY. clusterProfiler: an R package for comparing biological themes among gene clusters. *OMICS*. 2012;16(5): 284–287. <https://doi.org/10.1089/omi.2011.0118>.
23. Yu G, He QY. ReactomePA: an R/Bioconductor package for reactome pathway analysis and visualization. *Mol Biosyst*. 2016;12(2):477–479. <https://doi.org/10.1039/c5mb00663e>.
24. Sigdel T, Nguyen M, Liberto J, et al. Assessment of 19 genes and validation of CRM gene panel for quantitative transcriptional analysis of molecular rejection and inflammation in archival kidney transplant biopsies. *Front Med (Lausanne)*. 2019;6:213. <https://doi.org/10.3389/fmed.2019.00213>.
25. Sigdel TK, Yang JYC, Bestard O, et al. A urinary Common Rejection Module (uCRM) score for non-invasive kidney transplant monitoring. *PLoS One*. 2019;14(7):e0220052. <https://doi.org/10.1371/journal.pone.0220052>.
26. Drayton DL, Liao S, Mounzer RH, Ruddle NH. Lymphoid organ development: from ontogeny to neogenesis. *Nat Immunol*. 2006;7(4): 344–353. <https://doi.org/10.1038/ni1330>.
27. Kondo T, Morita K, Watarai Y, et al. Early increased chemokine expression and production in murine allogeneic skin grafts is mediated by natural killer cells. *Transplantation*. 2000;69(5):969–977. <https://doi.org/10.1097/00007890-200003150-00051>.
28. Obara H, Nagasaki K, Hsieh CL, et al. IFN-gamma, produced by NK cells that infiltrate liver allografts early after transplantation, links the innate and adaptive immune responses. *Am J Transplant*. 2005;5(9):2094–2103. <https://doi.org/10.1111/j.1600-6143.2005.00995.x>.
29. Zhao DXM, Hu Y, Miller GG, Luster AD, Mitchell RN, Libby P. Differential expression of the IFN- γ -inducible CXCR3-binding chemokines, IFN-inducible protein 10, monokine induced by IFN, and IFN-inducible T cell α chemoattractant in human cardiac allografts: association with cardiac allograft vasculopathy and acute rejection. *J Immunol*. 2002;169(3):1556–1560. <https://doi.org/10.4049/jimmunol.169.3.1556>.
30. Papadimitriou JC, Drachenberg CB. Distinctive morphological features of antibody-mediated and T-cell-mediated acute rejection in pancreas allograft biopsies. *Curr Opin Organ Transplant*. 2012;17(1):93–99. <https://doi.org/10.1097/MOT.0b013e31832834ee754>.
31. Drachenberg CB, Odorico J, Demetris AJ, et al. Banff schema for grading pancreas allograft rejection: working proposal by a multi-disciplinary international consensus panel. *Am J Transplant*. 2008;8(6):1237–1249. <https://doi.org/10.1111/j.1600-6143.2008.02212.x>.
32. Aziz F, Parajuli S, Uddin S, et al. How should pancreas transplant rejection be treated? *Transplantation*. 2019;103(9):1928–1934. <https://doi.org/10.1097/TP.0000000000002694>.
33. Burke GWIII, Chen LJ, Ciancio G, Pugliese A. Biomarkers in pancreas transplant. *Curr Opin Organ Transplant*. 2016;21(4):412–418. <https://doi.org/10.1097/MOT.0000000000000333>.